X-RAY COMPUTED TOMOGRAPHY OBSERVATIONS OF LOW-NOISE MIXES

J. ADRIEN
Mateis Laboratory, Insa de Lyon, France
Jerome.adrien@insa-lyon.fr
X. CARBONNEAU & V. LAPEYRONIE
Asphalt mixes Department, Campus for Science and technique, Colas, France
carbonneau@campus.colas.fr lapeyronie@campus.colas.fr

INTRODUCTION

In recent years, low-noise mixes have met with considerable success, as they provide an effective response to a well-identified problem and produced effects that are directly perceptible by residents. The design of mixes that reduce rolling noise is based on the presence of a high voids content. At the same time, there is a tendency to reduce the maximum particle size (D) without sacrificing skidding resistance which remains excellent even in the case of mixes with 0/4 mm aggregate. The focus of conventional mix design tools is on mechanical characteristics which is generally combined, in the case of low-noise mixes, with a measurement of absorption capacities. These methods provide only an overview of the product and knowledge of the voids content, but are unable to characterize the morphology of the voids. Computed tomography can reveal this morphology in detail. This observation technique was tested on ten different mixes. After a brief presentation of the technique and the information it can provide the paper describes the tested mixes and analyzes them in terms of their acoustic performance and the detailed characteristics of their void space.

1. COMPUTED TOMOGRAPHY OBSERVATIONS

X-ray computed tomography is a nondestructive technique for visualizing the interior of a material which would be opaque under optical mcroscopy. A very detailed description of the apparatus can be found in Maire et al. [1]. The X-ray beam passes through the sample and is captured by a dedicated detector which transforms it into an electrical signal then into numerical data. This provides a radiograph which is a projection of all the absorption coefficients of the structure. By rotating the sample perpendicular to the X-ray beam it is possible to collect N radiographs for N angular positions of the sample in the beam. A reconstruction algorithm [2] is then used to provide a precise map of the local absorption

coefficients (μ) throughout the volume of the sample which is divided into small cubic sub-elements known as voxels. As the value of μ is characteristic of the local composition of the material volume, imaging or surface imaging can be used to show the internal structure of a material.

This observation technique has gained in popularity recently as it provides a way of visualizing the internal structure of an object which previously could only be discovered from plane images of its surfaces or cross sections which were often limited in number. For bituminous materials, mention can be made of the recent research by Khan and Collop [3] which dealt with the observation and quantification of damage under mechanical stress by measuring the voids content as a function of the cumulative strain in the specimen. This technique has also been used to observe the changes that take place in the granular structure during compaction and in the number of intergranular contact points [4] as well as the uniformity of the binder in the case of a mix that includes recycled asphalt pavement [5].

Last, a study conducted at the University of Delft [6] used this technique to characterize the pore space of low-noise mixes. In this study, the observations were made on core samples taken from pavements and revealed a lower number of pore network connections in the samples taken from the traffic lanes than in those taken from untrafficked zones of the pavement. This change under traffic was blamed for the reduction in the low-noise qualities of the surfacing.

2. OBSERVATION METHOD

The tomograph in the MATEIS laboratory at INSA in Lyon was used for this study. It contains an X-ray tube whose voltage can be varied between 10 and 160 kV producing a maximum beam intensity of 840 μA. The X-ray source is polychromatic and generating a conical beam so it is easy to obtain a large range of resolutions by placing the sample at varying distances from the source and the detector. The resolution used for a scan was a compromise between the size of the sample and the resolution needed to observe the smallest elements.

A preliminary test was conducted on a compete specimen (a cylinder 100 mm long and 30 mm thick) at a resolution of 60 μm, a voltage of 160 kV and a beam intensity of 160 μA. The exposure time for each radiograph was 500 ms (with on average 3 radiographs from

each angle), 900 radiographs were taken for each sample as it was rotated through 360°. The total acquisition time was approximately 40 minutes.
Next, samples taken from the cylindrical specimens were analyzed in the same way but with a resolution of 17 µm, a voltage of 160 kV and a beam intensity of 160 µA□

Using the reconstructed cross-sections it was possible to quantify the voids in the material. This operation required several stages:

- application of a median 3D filter to attenuate the grey-level differences between adjacent voxels (noise reduction),
- thresholding in order to assign the same grey level to all the pores (binarization),
- computation of the variations in pore fractions in the 3 spatial directions. This provided the 3D distribution of the voids and the pore volume fraction,
- allocation of a different grey level to each pore zone (labelling),
- computation of the volume of each pore zone,
- computation of the connectivity, which is the ratio between the volume of the largest pore (the volume of the largest grouping of voxels) and the total pore volume.
- characterization of the size of pores and the characteristics of the inter-pore connectivity using a tool that applied erosion/dilation operations. This type of method was necessary in this case because of the highly interconnected nature of the cavities (each cavity is not an independent entity). Gradual erosion of the pore phase was conducted in the three directions of (X, Y and Z). Each pore which disappeared during erosion was labelled. The next operation was dilation that was proportional to the initial radius of the pore. Once the analysis was completed, this method made it possible to obtain the following: the coordinates of each pore centre, the number and size of pores that are adjacent to each pore and the number of voxels in the zones where two pores intersect.

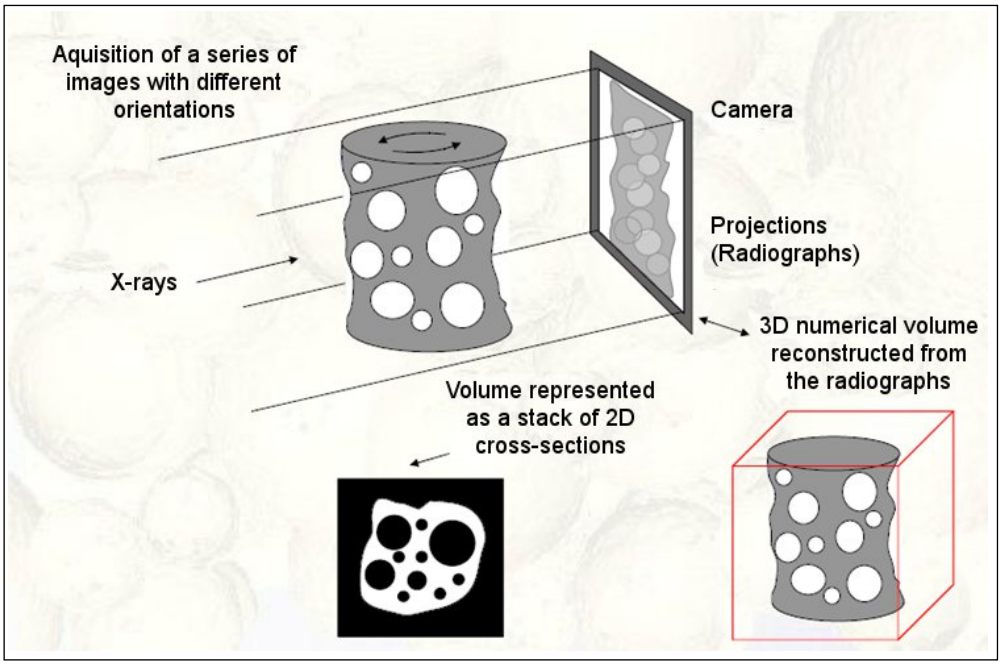

Figure 1 The principle of tomography

3. ANALYZED MIXES

The ten asphaltic mixes that were selected for this study reflect the most recent developments in high absorption mixes. They had maximum particle sizes of between 3 and 6 mm, and used straight or modified binders. Some incorporated additional materials, specific vacuolar materials or polystyrene beads. The main characteristics are set out in the table below:

Mix reference	D (mm)	K	Type of binder	Specific characteristics
A (090752)	4	4.05	Modified	
B (090499)	4	3.22	Modified	Pigment
C (090752)	4	4.40	Modified	Fibres
D (100596)	6	3.83	Modified	
E (100147)	5	3.37	Modified	Vacuolar material
F (091016)	6	3.57	Modified	
G (091016)	4	4.03	Modified	Fibres
H (100429)	3	4.50	Modified	Artificial aggregate
I (100785)	4	3.49	Modified warm	PS beads
J (100596)	6	3.72	Modified	

Table 1 Principal characteristics of the mixes selected for the study

The specifications of the mixes are familiar and acheivable. The size of the chippings and the proportion of each fraction were optimized to obtain products with a large pore space. The voids contents of these products were characterized by means of the Gyratory Shear Compaction Test (NF EN 12697-10 Compactability) that is able to cover void contents of between 15 and 30%. For some of these mixes modified Cantabro tests were also preformed on a batch of three specimens at a temperature of -10°C.

The modified Cantabro test measures a mix's sensitivity to aggregate stripping or shear when 3 samples are tumbled for 500 revolutions in a Los Angeles drum (test described in NF EN 12697-17 modified). After this erosion procedure the mass lost by the sample was measured.

Impedance tube tests were then conducted to measure the noise absorbing characteristics of each low-noise mix.

The impedance tube, or Kundt's tube, is a so-called two-microphone tube for measuring the acoustic absorption of a material placed inside it. A wide frequency range impedance tube was used to characterize the mixes over the 200Hz to 1600Hz frequency band (Figure 1).

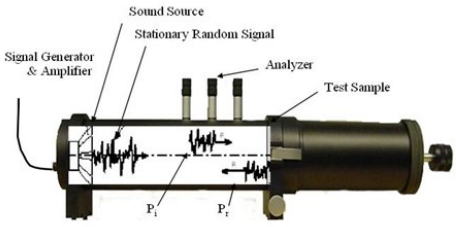

Transfer function between the two microphones

$$H_{12} = \frac{P_2}{P_1} = \frac{e^{jkh} + Re^{-jkh}}{e^{jk(h+s)} + e^{-jk(h+s)}}$$

h : distance between microphone and sample

k : wavenumber

s : distance between the 2 microphones

Reflection function

$$R = \frac{H_{12} - e^{-jks}}{e^{jks} - H_{12}} e^{j2k(h+s)}$$

Absorption coefficient

$$\alpha = 1 - |R|^2$$

Figure 2 An impedance tube with associated equations

The impedance tube's noise generator provided pink noise which was reflected from the sample located at the other end of the tube as shown in Figure 2. The response was then measured by two microphones positioned in front of the sample. A transfer function was applied in order to distinguish between the emitted signal and the reflected signal. The

absorption coefficient α was deduced from the pressure differences between the incident signal and the reflected signal.

The impedance tube was able to measure specimens with a diameter of 100 mm, for example Gyropac specimens or core samples, whose voids content is the same as that observed on site. The thickness was varied between 25 and 50mm in order to determine the optimum thickness that produces the largest possible dl(α) value. The coefficient dl(α) was then determined by weighting the coefficient α on the basis of the normalized traffic spectrum.

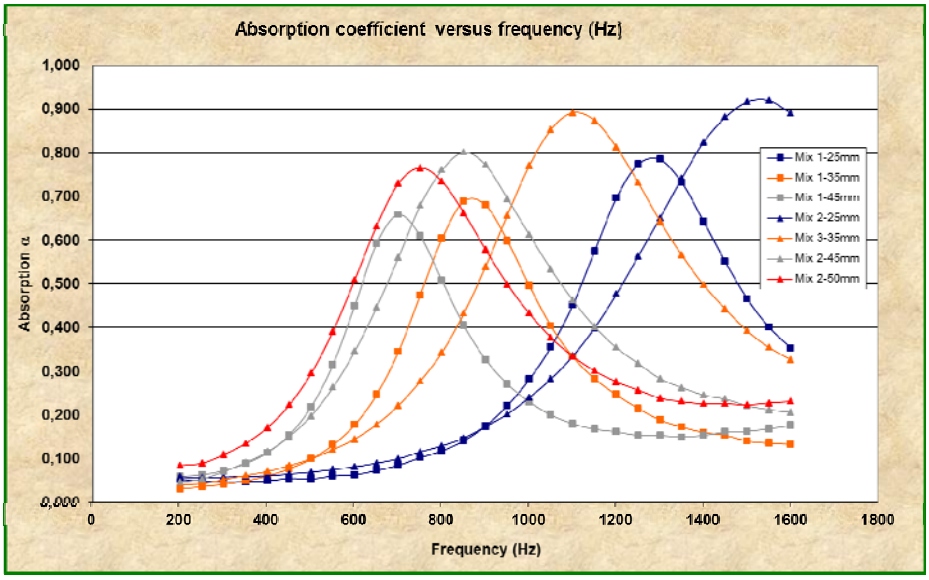

Figure 3 Example of measured signals: absorption coefficient as a function of frequency

As these spectra and the measurement method only provide the normal incidence absorption response, the term “pure” absorption can be applied. However, in the context of roads and tyre-pavement contact two other phenomena are apparent, namely generation and absorption in the propagation zones. These two phenomena can be quantified by means of CPX near-field measurements (XP S 31-145-1). The mixes we are concerned with are high-performance products that meet generation and absorption requirements in propagation zones.

The principal results obtained for the ten selected mixes are set out in the table below:

Mix reference	% voids – Gyratory Shear Compactor (200 gyrations)	% loss during Cantabro test (-10°C)	dLα max + corresponding voids content
A (090752)	25.6	20.7	3.1 (27.0)
B (090499)	23.5	/	2.8 (25.0)
C (090752)	20.1	/	2.1 (20,8)
D (100596)		/	1.6 (18.2)
E (100147)	21.9	19.2	2.7 (24.0)
F (091016)	26.3	24.1	2.9 (27.8)
G (091016)	25.5	17.9	2.9 (26.5)
H (100429)	26.0	36.6	3.2 (28.5)
I (100785)	22.2	/	2.8 (24.0)
J (100596)		/	2.0 (20.6)

Table 2 Principal characteristics determined for the selected mixes

In addition to the maximum absorption value given in Table 2, the way "dL(α)" varies according to the thickness of the sample for all the tested mixes is shown in Figure 4.

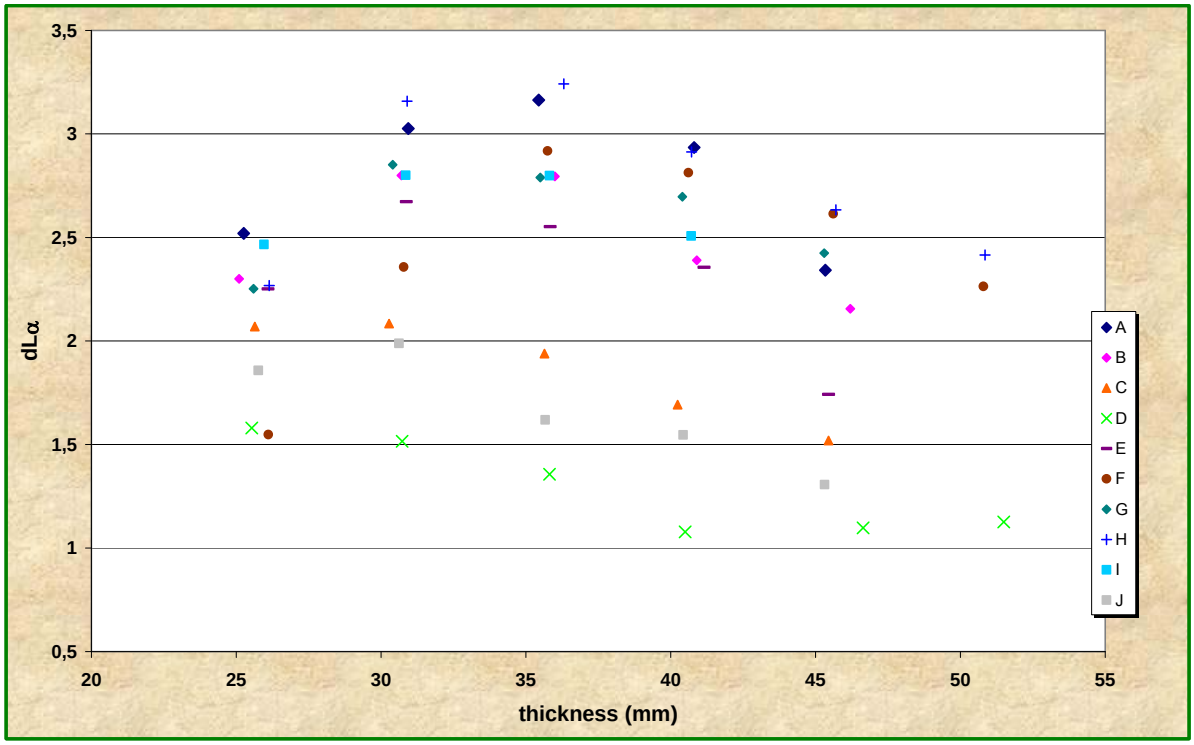

Figure 4 dL(α) according to thickness for each type of mix

For the thicknesses that are generally laid (between 30 and 40 mm), the maximum dL(α) values ranged between 1.5 and 3.1 dB(A). In the case of some low-noise mix designs the absorption coefficient is fairly independent of the thickness giving tolerances of between 5 and 10 mm while for others it varies a great deal.

The ten specimens fall into two major groups : mixes with excellent low-noise performance (A, B, E, F, G, H & I) with dLα max values of between 2.5 and 3.2 dB(A), and low noise mixes (C, D, J) with dLα max values of between 1.5 and 2.1 dB(A).

This figure also shows that behaviour varies with thickness in two distinct ways. Some mix designs, such as A, H and G, a fairly insensitive to variations in thickness. Their optimum absorption was retained with variations of 5 to 10 mm around the maximum. In contrast, variations in thickness produced a more marked change in the absorption properties of mixes B, C, E, F and I.

4. CHARACTERIZATION OF THE PORES USING TOMOGRAPHY

The samples used for the computed tomography observations were cut from the cylindrical specimens used for the absorption measurements. Prior to this, analysis of an entire specimen had shown that the Gyropac moulding of mixes with these particle size distributions produced completely homogeneous specimens, as can be seen in Figure 5 which shows the analyzed specimen with the variation in its voids content in 3 directions. This also confirms that the impedance tube measurements were made on flat homogeneous surfaces from which small samples could be cut in order to make higher resolution observations.

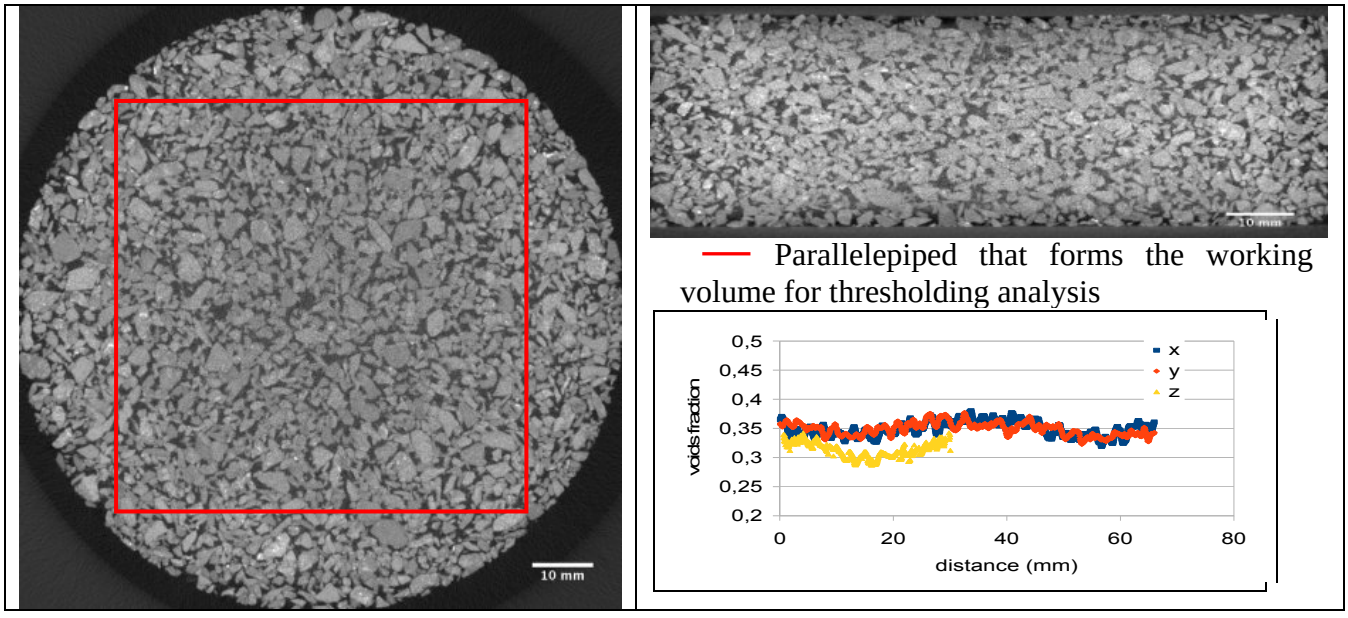

Figure 5 Image of the entire specimen and stability of the voids content after the compaction process

Figure 6 shows selected images that are representative of the microstructure of the 10 characterized mixes. The resolution was 17 μm.

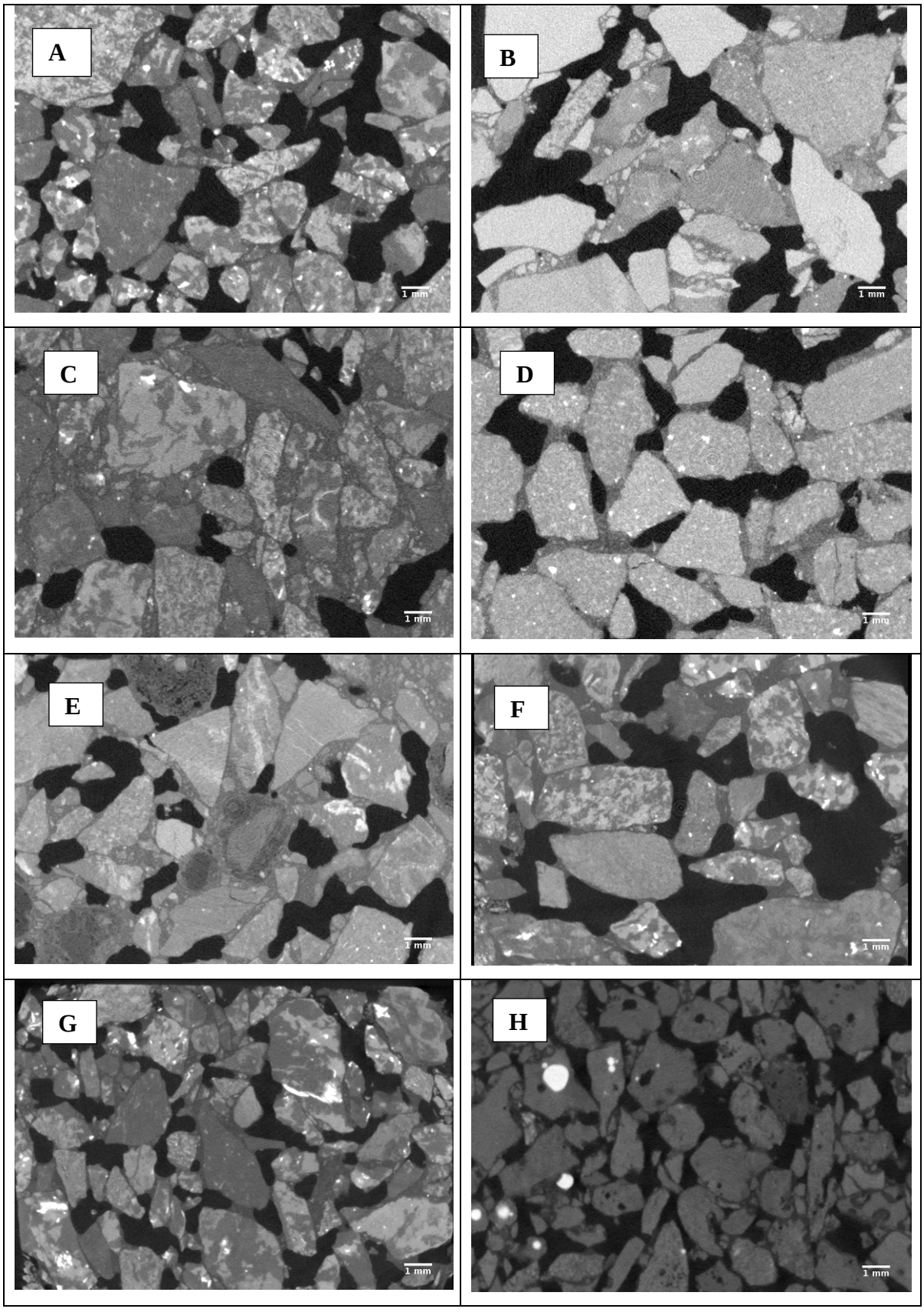

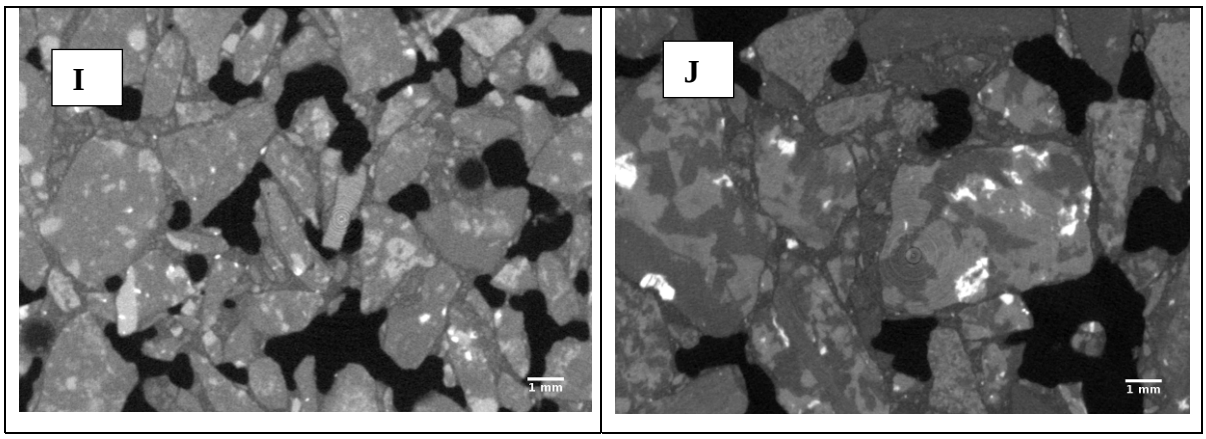

Figure 6 Images obtained from the different formulations characterized by computed tomography.

The contrast of these images is excellent which means the voids, which are the black areas, can be precisely quantified. The quality of the images also means we can see that in this type of mix the intergranular contact points are extremely small. Consequently, the characteristics of the binder, and more precisely those of the mastic which gives the mix its cohesion, will be essential for the durability of these formulations. These observations also demonstrate the new possibilities provided by recent reductions in mix manufacturing temperatures. For example, it can be seen that the polystyrene beads in mix I withstood both manufacture and compaction in the laboratory. They can be easily identified and retained their spherical shape. However, the contrast at their edge is fairly low which makes the precise determination of their outline more complex. In spite of this it is still possible to establish how they are distributed within the material, as can be seen in Figure 7.

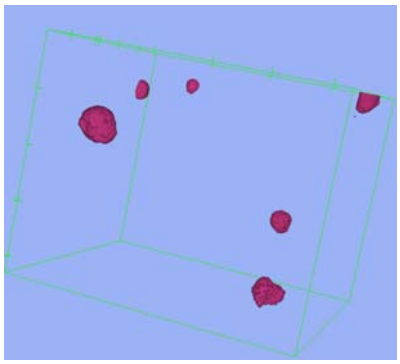

Figure 7 Image showing the spatial distribution of the polystyrene beads within the analyzed mix specimen

The average volumes analyzed at this level of resolution are given in Table 3. Using these specimens it is also possible to compute the voids content and the connectivity of the pore network. This reveals a particularity of the void network which is totally interconnected: starting from one pore it is possible to pass through all the pores in the mix.

Mix reference	Volume analyzed (mm^3)	Mean pore volume fraction from computed tomography	Pore connectivity
A (090752)	2948	24	0.98
B (090499)	2948	23	0.98
C (090752)	2986	14	0.74
D (100596)	2388	19	0.99
E (100147)	2751	21	0.97
F (091016)	1990	25	0.99
G (091016)	1533	22	0.99
H (100429)	1792	19.7	0.98
I (100785)	1505	17.5	0.98
J (100596)	2211	13.6	0.68

Table 3 General characteristics determined by computed tomography

All these mixes had a voids content of between 20 and 25%, with the notable exception of mixes C and J, which were, incidentally, the only two which did not have a completely communicating pore network.

5. ANALYSIS OF THE CHARACTERISTICS OF THE MIXES AND THE OBSERVATIONS

The following extrapolations were obtained from our X-ray computed tomography measurements and thresholding operations. Results are presented in figure 8.

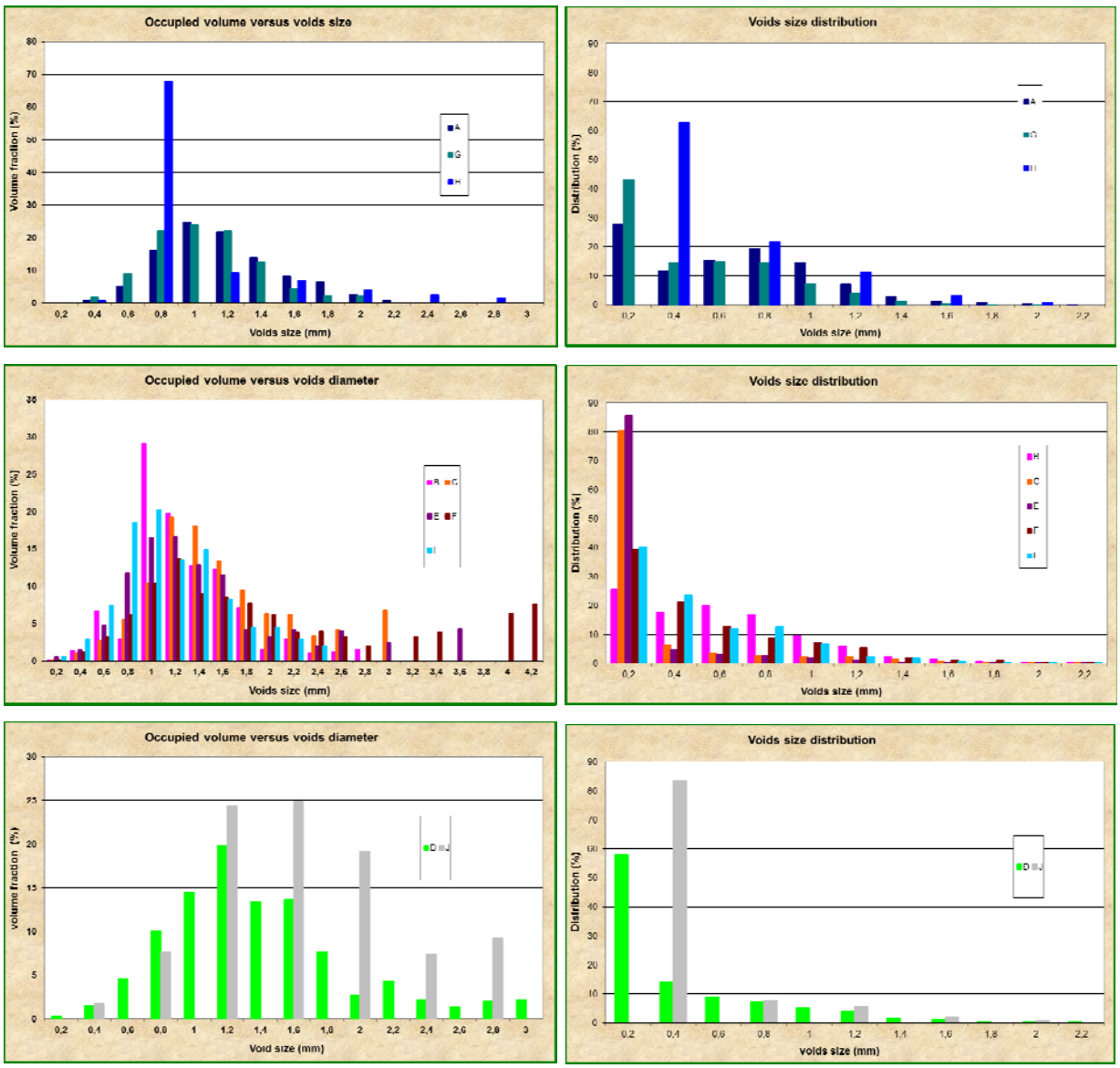

Figure 8 Voids size and distribution determined by X Ray tomograohy on all mixes

Following on from the previous conclusions provided by the DLα measurements, comparative measurements were made using X-ray computed tomography in order to quantify the size of the voids and their total volume. The 3 groups formed by mixes A, G and H, mixes B, C, E, F and I, and mixes D and J had different intrinsic characteristics. The measurements provide an approximate idea of the tortuosity of the pore network in the mixes.

The Figures show three types of material: in the first group the size of the voids is fairly uniform, between 0.2 and 1.0mm, and a major percentage of the void fraction (60%) is composed of voids measuring between 0.8 and 1.2mm.

The second group is characterized by a high proportion of fairly small voids (40 to 80%) and a fairly small amount of larger voids. However, this group may also contain a second type of void structure with between 20 and 40% of small voids (<0.4mm) and a moderate decrease in the number of voids up to 1.0mm. Between 60 and 80% of the total volume of these voids is taken up by voids of between 1.0 and 1.6mm.

In the last group, the majority of the voids are between 0.2 and 0.4mm. However voids measuring between 1.0 and 1.6mm or 1.2 and 2mm account for most of the total volume of voids.

At the present time this analysis remains very qualitative. It nevertheless shows the limits to the extent to which variations in the composition of the granular mixture, in terms of gradation cut-offs and particle size distribution, can modify the pore network in the mix after compaction. The reason for this is that currently all the mix designs that attempt to reduce rolling noise tend to have small particle sizes, typically approximately 6mm and down to 4mm in the case of some mixes that have been optimized for absorption. In addition to the initial performance, the way these mixes change under traffic must also be taken into account, as must the deterioration in their acoustic properties. Future optimization will no doubt involve improvements to the binders and/or the mastic more than major changes with regard to controlling the pore space.

CONCLUSION AND OUTLOOK

This research allowed us to conduct a preliminary observation of a large number of mixes that limit rolling noise and precisely quantify their pore space. Finding direct links between this geometric characterization and the acoustic properties remains very qualitative, and further interpretation of the data collected in this study is still needed. It nevertheless seems that the specially designed noise reducing mixes that have been considered here show that we have reached the physical limits as regards controlling the pore space. We cannot hope for significant progress from a change in particle size distributions and the choice of cut-off points. Future work must concentrate more on improving binders in order to guarantee that these mixes are durable under traffic and have lasting noise absorption properties. These small networks must also be assessed over a period of time to check

that they are not excessively affected by the accumulation of particles, which can be assessed with newly developed in-situ impedance tube measurement systems.

REFERENCES

1. Maire, E., Buffière, J. Y., Salvo, L., Blandin, J. J., Ludwig,W. and Letang M., On the application of X-ray microtomography in the field of materials science. J. Adv. Eng. Mater. 2001, 3(8), 539–546
2. Feldkamp L.A., Davis L.C. and Kress J.W., Practical cone beam algorithm, J. Opt. Soc. Am. A, 1984,1, p. 612-619
3. R. Khan, A.C. Collop, The use of X Ray Computed Tomography to characterize Microdamage in asphalt", Road Materials and Pavement design, EATA 2010, 89-109
4. M. Kutay, E. Arambula, N. Gibson, J Youtcheff, Three dimensional image processing methods to identify and characterise aggregates in compacted asphalt mixtures, International journal of pavement design, vol 11, N°6, December 2010, 511-528.
5. C. Druta, L. Wang, T. Zhu, Laboratory investigation of Reclaimed Asphalt Pavement mixed with pure binder using X-Ray CT Scanner, ICCTP 2009, Critical Issues in Transportation systems planning development and Management.

6 M. Van de Ven, W. Verwaal, A. Molenaar, Asphalt Material Characterization with(Nano)X-Ray Computerized Tomography, Procedings AES-TEMA 2009, Third international conference, Montreal, Canada, July 6-10 2009, 267-272.